14th International Conference on Applications of Statistics and Probability in Civil Engineering, ICASP14
Dublin, Ireland, July 9-13, 2023

Modified Cloud Analysis: An efficient tool for seismic fragility assessment.

Fatemeh Jalayer
Professor, Institute for Risk and Disaster Reduction (IRDR), University College London, London, UK

Hossein Ebrahimian
Assistant Professor, Dept. of Structures for Engineering and Architecture, University of Naples Federico II, Naples, Italy

ABSTRACT: Modified Cloud Analysis (MCA) is proposed as an alternative to the original Cloud Analysis for handling the collapse-inducing records. Collapse and non-collapse part of the data are treated as mutually exclusive and collectively exhaustive events. In this way, the original cloud analysis is applied to the non-collapse portion of the records. The collapse probability is modelled using a generalized regression model (logistic regression). Focusing on fragility assessment for a 3D structural model of an existing five-story RC building located in L'Aquila (central Italy), the present work provides a multi-faceted discussion of the Modified Cloud Analysis and its various applications in modern probabilistic performance-based earthquake engineering.

1. INTRODUCTION

Seismic fragility can be efficiently estimated by employing nonlinear dynamic analysis procedures, denoted herein as NDAP. Examples of NDAPs are: Incremental Dynamic Analysis (IDA), Multiple-Stripe Analysis (MSA), Cloud Analysis (CA) (see eg, Jalayer et al. 2017). Both IDA and MSA involve using a suite of ground motions scaled successively to higher levels of *IM*. MSA has the potential of using different suites of ground motion at different *IM* levels by means of using, e.g., conditional spectrum (eg, Ebrahimian et al. 2012). CA predicts structural performance for a suite of un-scaled ground-motion records and is based on fitting a linear regression model in the logarithmic scale to the pairs of either engineering demand parameter or damage measure and *IM* of interest (a.k.a., Cloud data). Modified Cloud Analysis procedure (MCA, Jalayer et al. 2017) is an alternative to the original Cloud Analysis for handling explicitly the collapse-inducing records. Collapse and non-collapse part of the data are treated as mutually exclusive and collectively exhaustive. In this way, the original CA is applied to the non-collapse portion of the records. Collapse probability can be modelled using a generalized regression model (logistic regression).

This paper aims to show that MCA is an effective and viable tool for non-linear dynamic analysis, fragility assessment, safety-checking, and IM selection even with a full three-dimensional nonlinear model of the RC frame and the infills. As a case-study, a 3-dimensional structural model of an existing five-story RC building with infills located in L'Aquila (central Italy) is used. The structure in question has collapsed due to a soft-story mechanism in the L'Aquila 2009 earthquake. We have explicitly considered the interaction between flexure, shear and the axial forces and the rigid end rotation due to bar slip in the nonlinear modelling of this building.

2. MODIFIED CLOUD ANALYSIS (MCA)

2.1. Basic definitions: Limit states

Four limit states are considered herein, namely, SLV-Infills (life-safety for infills), SLD (damage limitation), SLV (life safety) and SLC (near collapse). In this way, we separate the onset of different limit states in infills and RC frame

members. The above limit states on a column and infill element are shown in Figure 1(c, d). SLV-Infills takes place when the first infilled panel in the whole building reaches 50% of the peak strength in the descending branch on its backbone curve (this is a sign of life safety excursion). For RC frame members (beams and columns), and on the lateral component-based force-deformation response, SLC is defined as the point where a 20% drop in maximum resistance takes place. The onset of the SLV is defined with a deformation equal to 3/4th of that for the onset of SLC. The onset of SLD corresponds to the initiation of member yielding. The structural global collapse of the building can be reached if one of the following criteria takes place: (1) at least 50% of the columns in a story reach their ultimate deformational capacity (the component-level collapse, C, threshold is associated to the point having force equal to zero on the force-deformation backbone curve); (2) the drift of at least 50% of the columns in a story exceed 10%; (3) the maximum inter-story drift ratio measured at the center of mass of each story exceeds 10%; (4) the occurrence of global dynamic instability in the NRHA of the structure (manifest itself in the non-convergence issues in the finite element analysis software so that the analysis cannot be ended).

2.2. Basic definitions: Calculation of DCR_{LS}

MCA relies on employing a system-level damage measure expressed in a critical demand to capacity ratio (*DCR*) format. DCR_{LS} (for a given limit state *LS*) permits the mapping of damage at the component level to the system level (2017, and 2021; Miano et al. 2017, 2018); thus, a compatible definition is used for exceeding limit states at the component and system levels. For RC members, $DCR_{LS} = \max_j^N \left[D_j / C_j(LS)\right]$, where N is the number of components; D_j is the maximum absolute value of chord rotation response history over the time t (i.e., $\max_t\left[D_j(t)\right]$) evaluated for the j^{th} component; $C_j(LS)$ is the chord rotation capacity for the j^{th} component for the LS. It is apparent that at the onset of LS, $DCR_{LS} = 1.0$. It is to note that the positive and negative rotation capacities associated with $C_j(LS)$ are generally different for beam elements, which should be considered in calculating DCR_{LS}. The value DCR_C corresponds to the component-level collapse threshold, C. For the infills, $DCR_{\text{SLV-infills}} = \max_j^{N_{inf}} \left[\max^{n_{st}} \left(\boldsymbol{D}_j / C_j(LS)\right)\right]$, where N_{inf} is the total number of infill panels in the building; $\mathbf{D}_j$ is the vector of maximum values of axial compression strain response history over the time t evaluated for n_{st} struts of the j^{th} infill (herein, n_{st}=2); $C_j(LS)$ is the axial compression strain capacity for the j^{th} infill panel for the limit state SLV.

2.3. MCA procedure

Figure 2 presents a complete picture of MCA procedure using the DCR_{LS} as the damage measure (*LS*=SLC in this figure) versus *IM* for a set of *N* ground-motion records. Let *N* data be partitioned into two parts: (a) "*NoC* data" or "cloud data" represent the set of pairs [(*IM*, DCR_{LS})$^{(i)}$, i=1:N_{NoC}≤N] for which the structure does not collapse, i.e., related to N_{NoC} non-collapse inducing records (see orange-colored circles in Figure 2). (b) "*C* data" or "collapse data" correspond to the collapse-inducing records, i.e., those N_C records (where $N_{NoC}+N_C=N$) that cause global collapse of the structure (see red circles in Figure 2 lumped together at an arbitrary large *DCR* for the sake of illustration). The analytical fragility curve is non-lognormal expressed as a weighted sum of two terms: (1) *The* 3*-parameter CA-based lognormal fragility*: CA is applied to the *NoC* data with the weigh equal to the conditional probability of no-collapse *P*(*NoC*|*IM*); (2) *unity*: the probability of exceeding a *LS* given that collapse has taken place (see Eq. 1) weighted by the conditional probability of collapse *P*(*C*|*IM*)=1-*P*(*NoC*|*IM*). The term *P*(*C*|*IM*) is defined by a bi-parametric logistic regression model with the two parameters α_0 and α_1 (see Eq. 2). The MCA-based fragility assessment (FA) with five parameters $\boldsymbol{\chi}$=[a, b, $\beta_{DCR|S_a}$, α_0, α_1], is derived as (Jalayer et al 2017):

$$P\left(DCR_{LS}>1\middle|IM,\boldsymbol{\chi}\right)=\underbrace{\Phi\left(\frac{\ln\overbrace{\left(a\cdot IM^{b}\right)}^{\eta_{DCR|IM}}}{\beta_{DCR|IM}}\right)}_{\text{CA-based lognormal Fragility}}\times\underbrace{\left(\frac{e^{-\left(\alpha_0+\alpha_1\ln IM\right)}}{1+e^{-\left(\alpha_0+\alpha_1\ln IM\right)}}\right)}_{P\left(NoC|IM\right)}+1\times\underbrace{\left(\frac{1}{1+e^{-\left(\alpha_0+\alpha_1\ln IM\right)}}\right)}_{P\left(C|IM\right)=1-P\left(NoC|IM\right)} \quad (1)$$

where $\Phi(\cdot)$ is the standardized normal cumulative density function with the three parameters a, b, $\beta_{DCR|S_a}$; $\eta_{DCR|IM}=a\cdot IM^{b}$ and $\beta_{DCR|IM}$ are conditional median and logarithmic standard deviation of DCR_{LS} for *NoC* data. The median $\eta_{DCR|IM}$ for a prescribed *LS* is described as a power-law function indicating linear relation in logarithmic scale (see grey-dotted line labeled as "CA regression" in Figure 2). The p^{th} percentile of $DCR|IM$, at the intensity level x, denoted as $DCR^{p}(x)$, can be expressed as (see Jalayer et al. (2017) for the derivation):

$$DCR^{p}(x)=ax^{b}\exp\left(\beta_{DCR|IM}\Phi^{-1}\left[\frac{p}{P\left(NoC\mid IM\right)}\right]\right) \quad (2)$$

where $\Phi^{-1}(\cdot)$ is the inverse function of Φ. Eq. (2) is used herein to estimate the 16th, 50th and 84th percentile curves of $DCR|IM$. Figure 2 shows the curve DCR^{50} (p=50%) with thick dark-blue line labeled as "MCA regression", and the curves DCR^{16} and DCR^{84} with dashed-blue lines. To define an equivalent lognormal distribution for MCA-based fragility, the median at the onset of *LS*, $\eta_{IM|DCR=1}$, corresponds to DCR^{50}=1 (see the horizontal dash-dotted black line and the yellow cross in Figure 2, which corresponds to 50% probability of non-lognormal MCA-based fragility). The logarithmic standard deviation (dispersion) $\beta_{IM|DCR=1}$ of the equivalent lognormal fragility curve can be estimated as half of the logarithmic distance between *IM*'s corresponding to 16% and 84% probabilities (denoted as IM_C^{16} and IM_C^{84}) on the capacity curve (i.e., MCA-based fragility). $\beta_{IM|DCR=1}$ can also be estimated as half of the logarithmic distance between *IM*'s corresponding to DCR^{16}=1 and DCR^{84}=1 respectively, as illustrated with the green crosses on the vertical line DCR_{LS}=1.

The Robust Fragility (RF, Jalayer et al. 2017; Jalayer and Ebrahimian 2019) can be used to take into account the uncertainty in the MCA-based fragility model parameters $\boldsymbol{\chi}$ due to limited number of ground motions. RF is defined as the expected value for MCA-based fragility model considering the joint probability distribution for the fragility model parameters $\boldsymbol{\chi}$. Herein, we use an advanced simulation scheme (Jalayer et al. 2017) to generate samples from the 5 model parameters in $\boldsymbol{\chi}$. As a result, the RF and its certain confidence interval can be estimated. Overall effect of epistemic uncertainties can be seen through β_{UF} to be the logarithmic standard deviation. It is half of the (natural) logarithmic distance (along the *IM* axis) between the 84th and 16th percentile fragility curves, respectively (i.e., $\beta_{UF}=0.5\ln(IM^{84}/IM^{16})$, where IM^{84} and IM^{16} are *IM*'s at the median (50% probability) from the fragility minus/plus one standard deviation, respectively (see Figure 3). It is noted that β_{UF} can also take into account the modelling uncertainties in addition to uncertainty in the fragility model parameters. This condition can be met by using MCA in a one-to-one time-history/structural model realization coupling to efficiently propagate modelling uncertainties (see Jalayer and Ebrahimian 2019).

2.4. Safety-checking

Quantitative safety-checking is done using the IM-based Demand and Capacity Factor Design (DCFD, Jalayer and Cornell 2003, Jalayer et al. 2020), DCFD lends itself quite well to visual interpretation by comparing the seismic demand and capacity in probabilistic terms. The former *factored demand*, F_D accounts for the uncertainty in predicting the *IM* for an admissible risk level λ_a (related to the site-specific seismic hazard with its uncertainty associated with the considered *LS*); *Factored capacity*, F_C considers the uncertainty in predicting the *IM* capacity for a given *LS* (related to the fragility and its uncertainties $\beta_{IM|DCR=1}$ and β_{UF}). In a risk-based statement, $\lambda_{LS}\leq\lambda_a$ where λ_{LS} is the mean annual frequency of exceeding a

given *LS* (a.k.a. seismic risk). The *IM*-based DCFD is expressed as (Jalayer et al. 2020):

$$\underbrace{IM_{\lambda_a} \cdot \mathrm{e}^{\frac{k}{2}\beta_{UH}^2}}_{F_D} \leq \underbrace{\eta_{IM|DCR=1} \cdot \mathrm{e}^{\frac{-k}{2}\left(\beta_{IM|DCR=1}^2 + \beta_{UF}^2\right)}}_{F_C} \quad (3)$$

where IM_{λ_a} corresponds to the acceptable risk level λ_a through the median hazard curve λ_{IM} (the mean annual frequency of exceeding a given seismic intensity level); k is the slope of the linear approximation of λ_{IM} in the logarithmic scale (λ_{IM} is approximated by a power-law curve of the form $\lambda_{IM}(x) = k_o x^{-k}$, see Figure 3); β_{UH} represents the (equivalent) *IM*-based epistemic uncertainty related to hazard assessment (estimated as half of the logarithmic distance between hazard curves with 84% and 16% respectively along the *IM* axis, see Figure 6). The F_C parameters are defined in Section 1.3 considering that the *IM* at the onset of *LS* is expressed as a lognormal distribution with $\eta_{IM|DCR=1}$ and $\beta_{IM|DCR=1}$. It is noted that both the slope k and β_{UH} are estimated at the onset of *LS* (DCR_{LS}=1), i.e., $\eta_{IM|DCR=1}$. Safety Ratio, $SR = F_D/F_C \leq 1$, can be interpreted as a probabilistic quantification of the safety margin between system-level demand and capacity.

2.5. Efficiency and relative sufficiency measures using MCA procedure.

An efficient *IM* indicates that DCR_{LS} is well correlated with *IM*; thus, a relatively small number of records are required for a NDAP. Efficiency is measured in the literature as the conditional standard deviation of DCR_{LS} given *IM*, which, in the case of CA, is measured as $\beta_{DCR|IM}$ (Ebrahimian et al. 2015). Conditioning the damage measure DCR_{LS} directly on *IM* has the additional advantage of changing the metric of comparison from the structural response to measure of damage. This permits to quantify efficiency of an *IM* for a given limit state to be the dispersion of the MCA-based fragility curve $\beta_{IM|DCR=1}$. It is shown (Ebrahimian and Jalayer 2021) that $\beta_{IM|DCR=1}$ is more versatile (applicable to all NDAPs) with respect to $\beta_{DCR|IM}$ (the classic efficiency measure). Hence, an efficient *IM* may lead to more precise fragility curves (with smaller dispersion). It is to note that the use of $\beta_{IM|DCR=1}$ as a measure of efficiency will show some slight dependence on the limit state.

A sufficient *IM* renders the damage measure DCR_{LS} probabilistically dependent on the *IM* only, and not on the other ground-motion characteristics. Thus, it guarantees more accurate fragility estimate. Herein, the relative sufficiency measure (*RSM*, Jalayer et al. 2012) expressed in terms of DCR_{LS} and derived for MCA procedure on the basis of information theory (see Ebrahimian and Jalayer 2021). The *RSM*, denoted as $\mathrm{I}(DCR_{LS}|IM_2|IM_1)$ and measured in bits of information, quantifies the amount of information gained or lost on average about the designated DCR_{LS} by knowing IM_2 instead of IM_1 (relatively). It is approximated by averaging the relative entropy over a suite of real ground motion records. This provides a simple and fast screening tool for ranking various candidate *IM*s. The derived approximate formulation for *RSM* based on MCA is as follows (for brevity, DCR_{LS}=D):

$$\mathrm{I}\left(D\middle|IM_2\middle|IM_1\right) \approx \frac{1}{N_{NoC}} \sum_{k=1}^{N_{NoC}} \log_2 \frac{\phi\left(\ln\left(D_k/\eta_{D|IM_2}(k)\right)/\beta_{D|IM_2}\right) P\left(NoC\middle|IM_{2,k}\right) \beta_{D|IM_1}}{\phi\left(\ln\left(D_k/\eta_{D|IM_1}(k)\right)/\beta_{D|IM_1}\right) P\left(NoC\middle|IM_{1,k}\right) \beta_{D|IM_2}} \quad (4)$$

where $\eta_{D|IM_1}(k)$ and $\beta_{D|IM_1}$ are obtained from the CA-based regression on the cloud data={($IM_{1,k}$, D_k), k=1:N_{NoC}}; $\eta_{D|IM_2}(k)$ and $\beta_{D|IM_2}$ from the cloud data={($IM_{2,k}$, D_k), k=1:N_{NoC}}; $P(NoC|IM_{1,k})$ and $P(NoC|IM_{2,k})$ are the conditional probability of non-collapse estimated based on logistic regression model at $IM_{1,k}$ and $IM_{2,k}$, respectively (see Eq. 1).

3. NUMERICAL APPLICATION

3.1. Case-study model and ground-motion records

A five-story RC moment-resisting residential building with masonry infills, as shown in Figure 1(a, b), is considered as the case study. It was

constructed in the 1960s in L'Aquila (central Italy) and designed only for gravity loads. The structure was collapsed due to soft-story mechanism at 3rd floor in the L'Aquila 2009 earthquake. It lays on soil type B per the NTC 2018 with the average shear wave velocity of the upper 30m, V_{S30}=695m/s. The nonlinear modelling of the frame has been carried out using OpenSees version 3.3.0. The plasticity in structural elements is distributed over the plastic hinge length based on the force-based beam-column element (Beam with Hinges element) using the uniaxial Pinching4 material. The total lateral force-deformation response of the element considers the interaction between the shear, bar-slip, and the axial-flexural response. More details about this kind of nonlinear modelling of beam-column members can be found in Jalayer and Ebrahimian (2019) and Ebrahimian and Jalayer (2021).

For the infills, the model proposed by Liberatore et al. (2018) is used herein. According to this model, the shear versus horizontal displacement (or drift) backbone curve of infill is given by a multilinear curve defined by four characteristic points having different shear values, namely $0.40V_p$ (with V_p be the peak shear force), $0.85V_p$, V_p and zero. The effect of opening in infills is considered based on correction factor proposed by Decanini et al. (2014), assuming that the infills contain unreinforced opening. We use Pinching4 material for nonlinear modelling of the infill, and the equivalent strut is modeled by a Truss Element. Figure 1(c, d) illustrates the component-level limit states based on NTC 2018 (C8.7.1.3) including SLD (orange circle), SLV (magenta square) and SLC (red triangle) for RC beam-columns (see Figure 1c) and also SLV-infills (magenta triangle, see Figure 1d), as discussed previously in Sections 1.1 and 1.2. The point marked as (C) with red start in Figure 1c shows the component-level collapse threshold (see Section 1.2). With reference to the hysteretic response in Figure 1c, building has global structural collapse due to numerical instability in NRHA of record 71.

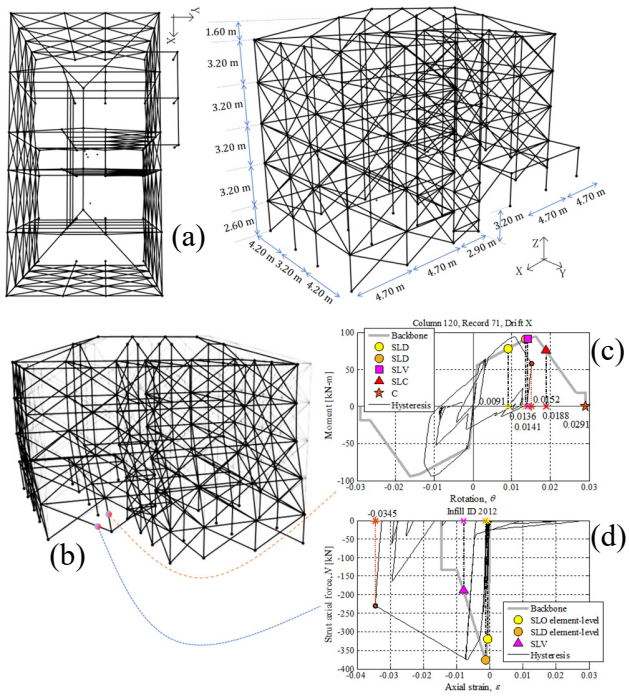

Figure 1: (a) Case-study building and the global axes; (b) final deformation of the case-study building subjected bidirectionally to M7.8 Turkey Earthquake 06 February 2023 KHMN (record 71 of the database); (c) the total monotonic moment-rotation response of column 120; (d) the axial force-strain of the equivalent truss element of the infill equivalent strut 2012 together with limit state thresholds and hysteretic responses for column and the infill equivalent strut(it is noted that the operational LS's SLO for frame, SLO- and SLD-infills are not considered in this study).

We have selected a large set of 81 ground-motion waveforms from different databases including: 57 records from NGA West2 (Ancheta et al. 2014); 11 from ITACA (Italian Accelerometric Archive, http://itaca.mi.ingv.it/) on the central Italy 2016 seismic sequence; 2 from International Institute of Earthquake Engineering and Seismology (IIEES, Dr. H. Zafarani, *personal communication*) on the Kermanshah M7.3 event; 11 from ESM (Engineering strong motion database, https://esm-db.eu/) including the February 2023 Turkey seismic sequence. These records have V_{S30}>360m/s (soil type B with a few on soil type A based on NTC 2018), M_w≥4.7, no limits on the source-to-site distance, and

correspond to crustal focal mechanisms (reverse, strike-slip and normal faulting styles).

3.2. MCA procedure: fragility assessment

Figure 2 shows the results of MCA procedure (see Section 1.3), where *LS*=SLC, for the complete set of records (*N*=81), and a smaller subset (*N*=10) of records from the original set of 81 waveforms (considering that seismic codes generally suggest the use of 7 to 10 records). The selection of 10 records from the 81 records set has been conducted just in a way that they cover a vast range of *IM* values and the data covers both sides of the line DCR_{LS}=1. Hence, no specific record selection strategy has been used for the subset of 10 records. The *IM*=*Sa*RotD50 which is 50th percentile (median) values of response spectra of the two horizontal components projected onto all nonredundant azimuths. This is in line with the definition of *IM* based on the ESHM20 hazard model (Danciu et al. 2021). In Figure 2, SaRotD50 is an abbreviation for the geometric mean of *IM* associated with the 1st- and 2nd-mode periods T_1=0.440sec, and T_2=0.351sec (i.e., $Sa_{\text{avg}}\text{RotD50}(T_1, T_2)$). Based on $\eta_{IM|DCR=1}$ and $\beta_{IM|DCR=1}$ reported in Figure 2, it is revealed that with careful record selection in the order suggested by the code, the fragility curve can be properly estimated using MCA procedure. Figure 3a shows the MCA-based RF curve for *N*=10 records (black solid line) with its standard deviation ($\pm 2\sigma$ confidence interval; shaded blue area), MCA-based FA (dashed red) for *N*=10, and (solid red) for *N*=81. The latter two are conventional approach of estimating the analytical fragility curve based on five-parameter model shown in Eq. (1). Both FA and RF fragilities for *N*=10 are almost identical (see Jalayer and Ebrahimian 2019). The large RF confidence band (due to 10 data) essentially indicate the error due to limited sample size. It contains the information regarding the record-to-record (RTR) variability. It is interesting to note that RF with its confidence band manages properly to capture MCA-based fragility based on the set of *N*=81 waveforms.

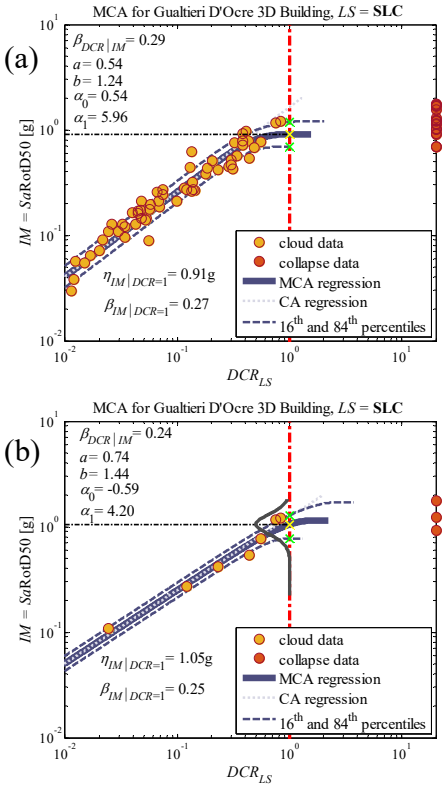

Figure 2: MCA procedure using (a) the set of 81 records, (b) a subset of 10 records.

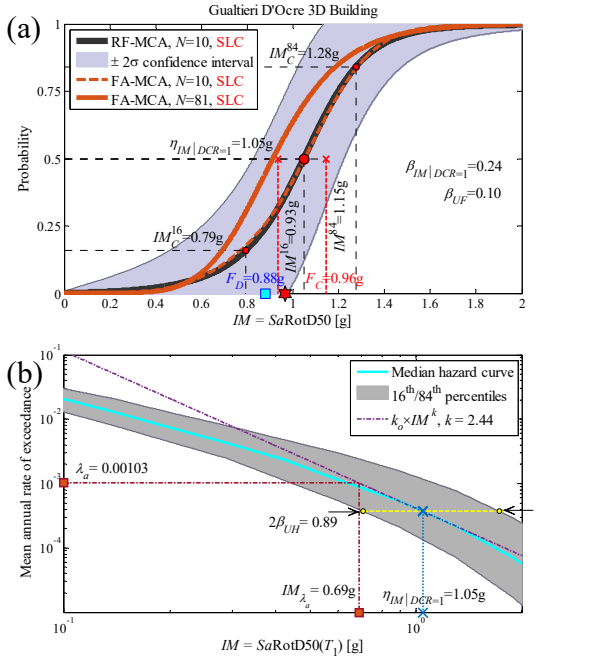

Figure 3: (a) Comparing the fragility curves for SLC limit state associated with N=81 and N=10 record sets; (b) site-specific median hazard curve with confidence interval.

3.3. MCA procedure: DCFD safety-checking

With reference to Section 1.4, IM_{λ_a}, k, and β_{UH} can be estimated visually from the site-specific hazard curve, λ_{IM}, and its 16th and 84th confidence interval (see Figure 3b, where we employed the ESHM20 hazard model for the building site). The hazard curve corresponds to $Sa\text{RotD50}(T_1 = 0.44\text{sec})$. The rate $\lambda_a = -\ln(1 - P_{V_R})/50C_U$, where $C_U = 1.0$ for residential buildings and the exceedance probability in the reference time period $50C_U$ years is $P_{V_R} = [0.63, 0.10, 0.05]$ for SLD, SLV and SLC limit state (NTC 2018), and $P_{V_R} = 0.10$ for SLV-infills; thus, $\lambda_a \cong 0.001$ for SLC (return period of around 975 years). The slope $k \cong 2.44$ and $\beta_{UH} \cong 0.45$ are estimated at $\eta_{IM|DCR=1} = 1.05g$ (for RF-MCA, *N*=10). Thus, $F_D = 0.69g \cdot \mathrm{e}^{2.44 \cdot 0.45^2/2} \cong 0.88g$. The fragility-based parameters $\eta_{IM|DCR=1}$, $\beta_{IM|DCR=1}$, and β_{UF} can be visually detected with reference to Figure 3a; thus, $F_C = 1.05g \cdot \mathrm{e}^{-2.44 \cdot (0.24^2 + 0.10^2)/2} \cong 0.96g$; thus, $SR = F_D/F_C \cong 0.90$. Both F_D and F_C values are visualized in Figure 3a, where it shows that the safety-checking criteria ($F_D \leq F_C$) is barely met for SLC limit state (in an engineering viewpoint, the building cannot be safe in SLC). Table 1 compares the *IM*-based safety-checking results based on MCA procedure on the two sets of records. It is seen that MCA-based DCFD safety-checking using a set of only 10 records give similar message, while it has considerable advantage in terms of computational effort. The cases which do not meet the safety-checking criteria (i.e., $F_D > F_C$) are highlighted, showing that SLV-Infills and also SLC limit states does not meet the safety-checking criteria. His message is signaled by even using the set of *N*=10 records.

Table 1: IM-based DCFD safety-checking results

Record set	DCFD terms	SLV-Infills	SLD	SLV	SLC
N=10	$F_D(g)$	0.552	0.195	0.552	0.878
	$F_C(g)$	0.398	0.556	0.709	0.965
	SR	1.39	0.35	0.78	0.91
N=81	$F_D(g)$	0.560	0.171	0.550	0.885
	$F_C(g)$	0.408	0.658	0.795	0.826
	SR	1.37	0.26	0.69	1.07

3.4. MCA procedure: ranking IMs

Using the efficiency and RSM (see Section 1.5), we want to rank three different *IM* including: (a) $Sa\text{RotD50} = Sa_{\text{avg}}\text{RotD50}(T_1, T_2)$ used herein for deriving the fragilities; (b) $Sa\text{RotD50}(T_1)$; (c) $Sa_{\text{avg}}\text{RotD50}(\mathbf{T} = [0.2T_1, 2T_1])$ with 20 equally-spaced points in the range of $[0.2T_1, 2T_1]$. Table 2 outlines the $\beta_{IM|DCR=1}$ as the measure for efficiency and $\mathrm{I}(DCR_{LS}|IM|IM_1)$ as the *RSM* of

of the considered *IM*s with respect to the reference $IM_1 = Sa\text{RotD50}$. We have used the complete set of records *N*=81 with relatively large number since the *RSM* is approximated by averaging the relative entropy over a suite of real ground motion records. With reference to Table 2, both efficiency and sufficiency show slight dependence on the *LS*. Moreover, $IM_3 = Sa_{\text{avg}}\text{RotD50}(\mathbf{T})$ has the highest (shown in blue) and $IM_2 = Sa\text{RotD50}(T_1)$ has the lowest (shown in red) ranks among the candidate *IM*s. For IM_3, $\beta_{IM|DCR=1}$ is the smallest for all the considered *LS*'s, which leads to more precise fragility estimate; its *RSM* estimated pairwise with respect to IM_1 is positive, which means that IM_3 gains more information about the uncertain parameter DCR_{LS} instead of IM_1. Vise versa, IM_2 has negative *RSM*, which reveals that information on DCR_{LS} is lost by adopting IM_2 instead of IM_1. This is generally not surprising; however, it shows the applicability of MCA procedure and the use of the approximate Eq. (4) for providing a screening tool to rank various candidate *IM*s.

Table 2: Ranking the three considered IMs

IM	Measure	SLV-Infills	SLD	SLV	SLC
IM_1	$\beta_{IM\|DCR=1}$	0.24	0.26	0.24	0.27
	$\mathrm{I}(DCR_{LS}\|IM_1\|IM_1)$	0.0	0.0	0.0	0.0
IM_2	$\beta_{IM\|DCR=1}$	0.29	0.27	0.25	0.29
	$\mathrm{I}(DCR_{LS}\|IM_2\|IM_1)$	-0.23	-0.07	-0.08	-0.14
IM_3	$\beta_{IM\|DCR=1}$	0.21	0.22	0.15	0.14
	$\mathrm{I}(DCR_{LS}\|IM_3\|IM_1)$	0.17	0.20	0.25	0.19

Note: $IM_1 = Sa\text{RotD50}$, $IM_2 = Sa\text{RotD50}(T_1)$, $IM_3 = Sa_{\text{avg}}\text{RotD50}(\mathbf{T})$

4. CONCLUSIONS

MCA, which employs un-scaled records, can be carried out with reasonable analysis effort (in the

order of 10 records) even for full three-dimensional nonlinear models of the RC frames and the infills. It can lead to very good fragility estimates if the ground motion records are chosen carefully. For the record selection, one should make sure that the suite of records covers a wide range of seismic intensity levels below and above *DCR*=1 for the desired limit states. It is shown that ranking adopted *IM*s by measuring their sufficiency and efficiency can be properly done in the light of MCA procedure. MCA can be effectively used for performance-based safety checking based on nonlinear time-history analysis.

5. ACNOWLEDGEMENTS

The authors would like to acknowledge partial support from the PRIN-2017 MATISSE (Methodologies for the AssessmenT of anthropogenic environmental hazard: Induced Seismicity by Sub-surface geo-resources Exploitation) project no. 20177EPPN2 funded by the Italian Ministry of Education and Research.

6. REFERENCES

Danciu, L., Nandan, S., Reyes, C., et al. (2021). *The 2020 update of the European Seismic Hazard Model: Model Overview*. EFEHR Technical Report 001, v1.0.0, DOI:10.12686/a15.

Ebrahimian H, Azarbakht A, Tabandeh A, Golafshani A. The exact and approximate conditional spectra in the multi-seismic-sources regions. *Soil Dyn Earthq Eng* 2012; 39, 61-77.

Ebrahimian H, Jalayer F, Lucchini A, Mollaioli F, and Manfredi G. (2015). Preliminary ranking of alternative scalar and vector intensity measures of ground shaking. *Bull Earthq Eng*, 13(10), 2805-2840.

Ebrahimian, H., and Jalayer, F. (2021) Selection of seismic intensity measures for prescribed limit states using alternative nonlinear dynamic analysis methods. *Earthq Eng Struct Dyn*, 50(5), 1235-1250.

Jalayer, F., and Cornell, C.A. (2003). *A technical framework for probability-based demand and capacity factor design (DCFD) seismic formats.* Tech. Rep. PEER2003/08, Pacific Earthquake Engineering Research Center (PEER), University of California Berkeley, CA.

Jalayer F, Beck J, and Zareian F (2012). Analyzing the sufficiency of alternative scalar and vector intensity measures of ground shaking based on information theory. *J Eng Mech,* 138(3), 307-316.

Jalayer, F., Ebrahimian, H., Miano, A., Manfredi, G., and Sezen, H. (2017). Analytical fragility assessment using unscaled ground motion records. *Earthq Eng Struct Dyn* 46(15):2639-2663.

Jalayer, F, and Ebrahimian, H. (2019) Seismic reliability assessment and the nonergodicity in the modelling parameter uncertainties. *Earthq Eng Struct Dyn,* 49(5), 434-457.

Jalayer, F., Ebrahimian, H., and Miano, A. (2020) Intensity-based demand and capacity factor design: A visual format for safety checking. *Earthquake Spectra*, 36(4), 1952-1975.

Jalayer, F., Ebrahimian, H., and Miano, A. (2021). Record-to-record variability and code-compatible seismic safety-checking with limited number of records. *Bull Earthq Eng*, 19(15), 6361-6396.

Miano, A., Jalayer, F., Ebrahimian, H., and Prota, A. (2018). Cloud to IDA: efficient fragility assessment with limited scaling. *Earthq Eng Struct Dyn*, 47(5), 1124-1147.

Miano, A. Ebrahimian, H. Jalayer, F., Vamvatsikos, D., and Prota, A. (2023). Propagation of modeling uncertainties for seismic risk asssessment: the effect of sampling techniques. *Earthq Eng Struct Dyn* (submitted).